Middle East Journal of Applied Science & Technology (MEJAST)
Volume 9, Issue 4, Pages 29-48, October-December 2026

Derivation and Applications of Optimization-Based Numerical Method for Solving Physical Real-Life Problems in Science and Engineering Modelled as Ordinary Differential Equations

Sabo John[1*], Dedan Gideon[2], Nathaniel Danladi[3], Hannatu Samuel[4] & Nkanga, Uboho Sunday[5]

[1,2]Department of Mathematics, Adamawa State University, Mubi, Nigeria. [3]Department of Mathematics, Modibbo Adama University, Yola, Nigeria. [4]Federal University Gashua, Yobe State, Nigeria. [5]Department of Mathematics, University of Abuja, FCT, Nigeria.
Corresponding Author (Sabo John) Email: sabojohn630@gmail.com[*]

DOI: Under Assignment

Copyright © 2026 Sabo John et al. This is an open-access article distributed under the terms of the Creative Commons Attribution License, which permits unrestricted use, distribution, and reproduction in any medium, provided the original author and source are credited.

Article Received: 20 August 2026 *Article Accepted: 27 October 2026* *Article Published: 29 October 2026*

ABSTRACT

This study presents the development and implementation of an Optimization-Based Numerical Method (OBNM) designed to solve modelled physical real life ordinary differential equations (ODEs) that emerge in scientific and engineering applications. The approach is constructed through a power series polynomial approximation involving interpolation and collocation techniques, where the degree of accuracy depends on the chosen number of interpolation and collocation points. By minimizing the truncation error, an optimized point is identified, resulting in a continuous formulation that, when evaluated at specific grid points, generates a block hybrid method. Key theoretical characteristics of the scheme are derived and examined, including order, error constant, consistency, zero-stability, convergence and absolute stability. The method is proven to be consistent, zero-stable, convergent and A-stable, with its absolute stability region encompassing the entire left half of the complex plane. The OBNM is subsequently tested on some practical ODEs models: Newton's law of cooling, radioactive decay, drug elimination, water heating and capacitor charging. Absolute errors are determined by comparing numerical approximations against exact analytical solutions, with outcomes displayed in tables and figures. In all five cases, the absolute errors fall within the range of double-precision machine round-off, indicating that the OBNM reproduces analytical solutions with essentially exact accuracy. Consequently, the method is demonstrated to be a dependable, stable and computationally efficient instrument for addressing first-order ODEs in scientific and engineering applications.

Keywords: Optimization-Based Numerical Method; Ordinary Differential Equations; Interpolation And Collocation; Consistent; Zero-Stability; Absolute Stability; Convergence; Absolute Error; Radioactive Decay; Drug Elimination; Water Heating; Capacitor Charging.

1.0. Introduction

Ordinary differential equation (ODE) solutions are used by scientists and engineers to model real-world phenomena in a variety of scientific, engineering, and industrial fields, such as reaction kinetics, heat transfer, and transport phenomena. However, exact analytical solutions are only available for simple or idealized cases, and practical problems require numerical methods because of their nonlinear, stiff and analytically intractable characteristics.

In order to improve convergence and lower computational error while providing reliable approximations of complicated ODE models, optimization-based numerical techniques have become especially crucial (Butcher, 2016; Abdelrahim et al., 2016). First-order ODEs are used to describe a variety of real-world processes, such as Newton's Law of Cooling, radioactive decay, drug elimination, heating of water, and capacitor charging. These ODEs demand precise and efficient numerical methods to solve (Adewale et al., 2024; Saha et al., 2025). Thus, an Optimization-Based Numerical Method (OBNM) utilizing power series polynomials through interpolation and collocation processes is presented in this work. The order of accuracy is determined by the number of interpolation and collocation points.

Numerical analysis and applied mathematics have shown a great deal of interest in the study of exponential growth and decay events in a variety of scientific fields, and researchers are creating increasingly complex solutions. Saha

et al., (2025) examined the analytical solution of fractional Newton's law of cooling in heat transfer applications using the Kushare transform, while Peker and Uysal (2024) investigated the application of the new general integral transform. Both studies show the ongoing significance of cooling models and the continuous efforts to develop more advanced solution techniques. The work of Alzaid et al., (2022) on Ralston's cubic convergence method and Kumar et al., (2024) on fractional differential equations has also advanced population growth modeling, demonstrating how sophisticated numerical techniques can accurately capture exponential growth characteristics while taking memory effects into account through fractional calculus frameworks. Malins and Lemoine (2022) created radioactivedecay, a Python package for radioactive decay calculations in nuclear science and pharmacokinetics, while Widodo and Indarsih (2020) used nonstandard finite difference methods to study drug elimination, highlighting the significance of trustworthy numerical tools in managing decay processes.

Industrial chemistry, applied physics, and engineering rely on ordinary differential equations derived from mass balance, rate laws, and physical principles such as Newton's law of cooling, with pseudo-first-order reactions, consecutive reaction mechanisms, and transient heat transfer problems serving as benchmark systems for testing numerical methods (Atkins & de Paula, 2014). These applications demonstrate how coupled dynamics, multiple time scales, and parameter sensitivity create challenges that reduce the capacity of classical numerical schemes to produce accurate and stable results, necessitating robust numerical algorithms capable of delivering dependable solutions for scientific research and engineering design (Sabo et al., 2024). This study therefore employs an optimized numerical method to solve benchmark problems from chemistry, physics, and applied mathematics, evaluating its performance against analytical solutions through accuracy, stability, and computational efficiency assessments presented in tabular and graphical form. The Optimization-Based Numerical Method successfully solves both single and coupled ODE problems, making it an effective solution for scientific and engineering applications.

The approach demonstrates how optimization-based numerical methods can enhance solution accuracy through its combination of high accuracy and stability and computational efficiency for solving complex real-world ODE models of the form:

$$\frac{d\gamma}{dt} = f(t, \gamma), \gamma(t_0) = \gamma_0 \tag{1.1}$$

Ahmad (2020) reviews numerical methods for multi-objective and constrained optimization in engineering, covering Pareto optimality, objective weighting, constraint formulations, and fuzzy set approaches, while emphasizing deterministic and stochastic algorithms, Lagrange multipliers, and sensitivity analysis for solving electromagnetic and engineering design problems; however, the work is largely descriptive with few mathematical proofs, limiting reproducibility and practical application. Petrović et al., (2025) provide an editorial synthesis of ten studies on numerical analysis and optimization, addressing monotone inclusion, neural network-based optimization, differential evolution, conjugate gradient methods, penalty techniques, and network equilibrium models, demonstrating the continued vitality of optimization techniques for complex scientific and engineering challenges while serving as an entry point for researchers exploring current developments.

The literature examines numerical optimization techniques and their practical applications. Gavin (2019) distinguishes search-based from gradient-based constrained optimization methods and explains how penalty functions convert constrained problems into unconstrained equivalents. Aljassas and Al-Jilawi (2023) analyze Newton's method for nonlinear problems, noting its rapid convergence but dependence on initial value selection, while Chan et al., (2025) implement the Newton-Raphson method in Python for ODEs, achieving high accuracy and fast convergence despite challenges with error accumulation and stiffness. Recent work advances hybrid block methods: Yakubu and Sibanda (2025) developed a one-step optimized hybrid block method for second-order ODEs with high-order accuracy and two stability types; Akinnukawe (2025) develops a two-step hybrid block approach for third-order initial value problems with superior accuracy and speed; and Gbenro (2025) introduces optimized and modified hybrid block methods for first-order ODEs that minimize truncation errors and CPU time. Collectively, these studies demonstrate how traditional, contemporary, and hybrid block schemes enhance stability, convergence, and computational efficiency across engineering and scientific applications (Yakubu & Sibanda, 2025; Akinnukawe, 2025; Gbenro, 2025).

1.1. Study Objectives

Based on the study, here are five research objectives:

1) To derive an Optimization-Based Numerical Method (OBNM) for solving first-order ordinary differential equations using a power series polynomial approximation via interpolation and collocation procedures.

2) To determine the optimal point by minimizing the truncation error, thereby yielding a continuous formulation that generates a block hybrid method when evaluated at selected grid points.

3) To establish the theoretical properties of the method, including its order and error constant, consistency, zero-stability, convergence and region of absolute stability.

4) To apply the OBNM to five real-life first-order ODE models Newton's law of cooling, radioactive decay, drug elimination, heating of water and capacitor charging and compare the approximate solutions with their analytical counterparts.

5) To evaluate the accuracy, stability and computational efficiency of the OBNM through absolute error analysis and graphical comparisons, in order to assess its reliability as a tool for solving first-order ODEs in scientific and engineering contexts.

2.0. Derivation of Optimization-Based Numerical Method (OBNM)

In this section, the derivation of Optimization-Based Numerical Method (OBNM) was carryout using the power series as a basis function through interpolation and collocation procedures.

Consider an approximate solution of a power series polynomial of the form;

$$\gamma(t) = \sum_{i=0}^{\omega+\varpi-1} \vartheta_j t^j \tag{2.1}$$

where ω and ϖ are the number of interpolation and collocation points respectively. The first derivative of (2.1) is given by

$$\gamma'(t)=\sum_{i=0}^{\omega+\varpi-1} j\vartheta_j t^{j-1} \tag{2.2}$$

where $\vartheta_j \in \Re$ for $j=0(1)6$ and $\gamma(t)$ is continuously differentiable. Let the solution of (1.1) be sought on the integration interval $[u,v]$ with a constant step-size h, defined by, $h=t_{n+1}-t_n$, $n=0,1,\cdots,N$ Substituting equation (2.2) in (1.1) to gives,

$$f(t,\gamma)=\sum_{i=0}^{\omega+\varpi-1} j\vartheta_j t^{j-1} \tag{2.2}$$

Therefore, interpolate equation (2.1) at point $t_{n+u}, u=0$ and collocate equation (2.2) at points $t_{n+v}, v=0,\xi,\frac{2}{5},\frac{3}{5},\frac{4}{5},1$, where ξ is the point of optimization. This leads to the following system of equations,

$$\begin{bmatrix} 1 & t_n & t_n^2 & t_n^3 & t_n^4 & t_n^5 & t_n^6 \\ 0 & 1 & 2t_n & 3t_n^2 & 4t_n^3 & 5t_n^4 & 6t_n^5 \\ 0 & 1 & 2t_{n+\xi} & 3t_{n+\xi}^2 & 4t_{n+\xi}^3 & 5t_{n+\xi}^4 & 6t_{n+\xi}^5 \\ 0 & 1 & 2t_{n+\frac{2}{5}} & 3t_{n+\frac{2}{5}}^2 & 4t_{n+\frac{2}{5}}^3 & 5t_{n+\frac{2}{5}}^4 & 6t_{n+\frac{2}{5}}^5 \\ 0 & 1 & 2t_{n+\frac{3}{5}} & 3t_{n+\frac{3}{5}}^2 & 4t_{n+\frac{3}{5}}^3 & 5t_{n+\frac{3}{5}}^4 & 6t_{n+\frac{3}{5}}^5 \\ 0 & 1 & 2t_{n+\frac{4}{5}} & 3t_{n+\frac{4}{5}}^2 & 4t_{n+\frac{4}{5}}^3 & 5t_{n+\frac{4}{5}}^4 & 6t_{n+\frac{4}{5}}^5 \\ 0 & 1 & 2t_{n+1} & 3t_{n+1}^2 & 4t_{n+1}^3 & 5t_{n+1}^4 & 6t_{n+1}^5 \end{bmatrix} \begin{bmatrix} \vartheta_0 \\ \vartheta_1 \\ \vartheta_2 \\ \vartheta_3 \\ \vartheta_4 \\ \vartheta_5 \\ \vartheta_6 \end{bmatrix} = \begin{bmatrix} \gamma_n \\ f_n \\ f_{n+\xi} \\ f_{n+\frac{2}{5}} \\ f_{n+\frac{3}{5}} \\ f_{n+\frac{4}{5}} \\ f_{n+1} \end{bmatrix} \tag{2.3}$$

Solving for equation (2.3) for $\vartheta_j's,\ j=0(1)6$ and substitute back into (2.1) to gives a optimized linear multistep hybrid method of the form

$$\gamma(t)=\alpha_0(t)\gamma_n+h\left[\beta_0(t)f_n+\beta_\xi(t)f_{n+\xi}+\beta_{\frac{2}{5}}(t)f_{n+\frac{2}{5}}+\beta_{\frac{3}{5}}(t)f_{n+\frac{3}{5}}+\beta_{\frac{4}{5}}(t)f_{n+\frac{4}{5}}+\beta_1(t)f_{n+1}\right] \tag{2.4}$$

Simplify equation (2.4) to gives

$$\left.\begin{aligned} \alpha_0(t)&=1 \\ \beta_0(t)&=\frac{1}{2016}\frac{217\xi-19}{\xi} \\ \beta_\xi(t)&=\frac{19}{84(\xi-1)(5\xi-3)(5\xi-4)(5\xi-2)} \\ \beta_{\frac{2}{5}}(t)&=\frac{25}{1008}\frac{105\xi-23}{5\xi-2} \\ \beta_{\frac{3}{5}}(t)&=-\frac{25}{504}\frac{35\xi-9}{5\xi-5} \\ \beta_{\frac{4}{5}}(t)&=\frac{25}{672}\frac{35\xi-9}{5\xi-4} \\ \beta_1(t)&=-\frac{1}{504}\frac{21\xi-2}{\xi-1} \end{aligned}\right\} \tag{2.5}$$

Now, substitute equation (2.5) into (2.3), after some simplifications, substitute the results one by one into (2.3) to gives

$$-\frac{1}{75600000}(190\xi - 27) = 0 \tag{2.6}$$

Solving for ξ in equation (2.6) to obtain the exact value of ξ as

$$\xi = \frac{27}{190} \tag{2.7}$$

Therefore, substitute equation (2.7) into (2.4) to gives new continuous form of OBNM as

$$\left.\begin{aligned}
&\alpha_0(t) = \tau \\
&\beta_0(t) = -\frac{\tau^2}{54432}\left(-27216 + 122052\tau - 271915\tau^2 + 322980\tau^3 - 195650\tau^4 + 4750\tau^5\right) \\
&\beta_{\frac{27}{190}}(t) = \frac{\tau^2}{54432}\left(336 - 1078\tau + 1491\tau^2 - 980\tau^3 + 250\tau^4\right) \\
&\beta_{\frac{2}{5}}(t) = -\frac{25t^3}{49392}\left(4536 - 24843\tau + 44310\tau^2 - 33810\tau^3 + 9500\tau^4\right) \\
&\beta_{\frac{3}{5}}(t) = \frac{25\tau^3}{43848}\left(3024 - 17822\tau + 36561\tau^2 - 31150\tau^3 + 9500\tau^4\right) \\
&\beta_{\frac{4}{5}}(t) = -\frac{\tau^3}{3360}\left(2268 - 13839\tau + 30408\tau^2 - 28490\tau^3 + 9500\tau^4\right) \\
&\beta_1(t) = \frac{\tau^3}{82152}\left(9072 - 56490\tau + 129255\tau^2 - 129150\tau^3 + 47500\tau^4\right)
\end{aligned}\right\} \tag{2.8}$$

where

$$\tau = \frac{t - t_n}{h} \tag{2.9}$$

Evaluate equation (2.4) at points $\left[\frac{27}{190}, \frac{2}{5}, \frac{3}{5}, \frac{4}{5}, 1\right]$ to obtain an Optimization-Based Numerical Method (OBNM) of the form

$$\mathrm{K}^{(0)}\mathrm{X}_m = \Omega\gamma_n + h\psi F(\gamma_n) + h\vartheta F(\mathrm{X}_n) \tag{2.10}$$

Where

$$\mathrm{X}_n = \left[\gamma_{n+\frac{27}{190}} \quad \gamma_{n+\frac{2}{5}} \quad y_{n+\frac{3}{5}} \quad \gamma_{n+\frac{4}{5}} \quad \gamma_{n+1}\right]^T, \gamma_n = \left[\gamma_{n-\frac{27}{190}} \quad \gamma_{n-\frac{2}{5}} \quad \gamma_{n-\frac{3}{5}} \quad \gamma_{n-\frac{4}{5}} \quad \gamma_n\right]^T$$

$$F(\mathrm{X}_n) = \left[f_{n+\frac{27}{190}} \quad f_{n+\frac{2}{5}} \quad f_{n+\frac{3}{5}} \quad f_{n+\frac{4}{5}} \quad f_{n+1}\right]^T, F(\gamma_n) = \left[f_{n-\frac{27}{190}} \quad f_{n-\frac{2}{5}} \quad f_{n-\frac{3}{5}} \quad f_{n-\frac{4}{5}} \quad f_n\right]^T$$

$$\mathrm{K}^{(0)}=\begin{bmatrix}1&0&0&0&0\\0&1&0&0&0\\0&0&1&0&0\\0&0&0&1&0\\0&0&0&0&1\end{bmatrix},\Omega=\begin{bmatrix}0&0&0&0&1\\0&0&0&0&1\\0&0&0&0&1\\0&0&0&0&1\\0&0&0&0&1\end{bmatrix},\psi=\begin{bmatrix}0&0&0&0&\frac{8352390951}{158470336000}\\0&0&0&0&\frac{787}{20250}\\0&0&0&0&\frac{737}{9000}\\0&0&0&0&\frac{1186}{30375}\\0&0&0&0&\frac{29}{648}\end{bmatrix}$$

$$\vartheta=\begin{bmatrix}\frac{5916138237}{55010462500}&-\frac{27030145581}{776504646400}&\frac{280954413}{11489099360}&-\frac{36774910197}{3961758400000}&\frac{4816554759}{3228833096000}\\\frac{13628448896}{58629571875}&\frac{1762}{11025}&-\frac{6}{145}&\frac{223}{18750}&-\frac{302}{183375}\\\frac{1446041816}{6514396875}&\frac{2601}{9800}&\frac{17}{232}&-\frac{27}{12500}&\frac{9}{163000}\\\frac{40568406016}{175888715625}&\frac{2584}{11025}&\frac{832}{3915}&\frac{818}{9375}&-\frac{704}{183375}\\\frac{19808792}{93807315}&\frac{1025}{3528}&\frac{25}{232}&\frac{17}{60}&\frac{733}{11736}\end{bmatrix}$$

3.0. Fundamental Properties of an Optimization-Based Numerical Method (OBNM)

This section presents the fundamental/theoretical properties of an Optimization-Based Numerical Method (OBNM). These properties are order and error constant, consistent, convergent, zero-stability and region of absolute stability of Optimization-Based Numerical Method (OBNM).

3.1. Order and Error Constant of OBNM

Consider the linear operator $L\{\gamma(t);h\}$ associated with optimization method be defined as,

$$L\{\gamma(t);h\}=\mathrm{K}^{(0)}\mathrm{X}_m=\Omega\gamma_n+h\psi F(\gamma_n)+h\vartheta F(\mathrm{X}_n) \tag{3.1}$$

Where d is the order of differential equation (Akinfenwa et al., 2020). Expanding (3.1) by Taylor series and comparing the coefficients of yield,

$$L\{\gamma(t);h\}=c_0\gamma(t)+c_1h\gamma'(t)+c_2h^2\gamma''(t)+\cdots+c_ph^p\gamma^p(t)+\cdots c_{p+1}h^{p+1}\gamma^{p+1}(t)+\cdots \tag{3.2}$$

Definition 3.1: let be the linear operator with the related continuous method (3.1) are supposed to be of order p if $c_0=c_1=c_2=\cdots=c_p=0$ and $c_{p+1}\neq 0$. c_{p+1} is refers to the error constant and the truncation error is known by

$$t_{n+k}=c_{p+1}h^{(p+1)}(x_n)+0(h^{p+2}) \tag{3.3}$$

Applying definition 3.1 on OBNM, we have

$$L\{\gamma(t);h\}=\begin{bmatrix}1&0&0&0&0\\0&1&0&0&0\\0&0&1&0&0\\0&0&0&1&0\\0&0&0&0&1\end{bmatrix}\begin{bmatrix}\gamma_{n+\frac{27}{190}}\\ \gamma_{n+\frac{2}{5}}\\ y_{n+\frac{3}{5}}\\ \gamma_{n+\frac{4}{5}}\\ \gamma_{n+1}\end{bmatrix}-\begin{bmatrix}0&0&0&0&1\\0&0&0&0&1\\0&0&0&0&1\\0&0&0&0&1\\0&0&0&0&1\end{bmatrix}\begin{bmatrix}\gamma_{n-\frac{27}{190}}\\ \gamma_{n-\frac{2}{5}}\\ \gamma_{n-\frac{3}{5}}\\ \gamma_{n-\frac{4}{5}}\\ \gamma_{n}\end{bmatrix}-$$

$$h\begin{bmatrix}\frac{8352390951}{158470336000}&\frac{5916138237}{55010462500}&-\frac{27030145581}{776504646400}&\frac{280954413}{11489099360}&-\frac{36774910197}{3961758400000}&\frac{4816554759}{3228833096000}\\ \frac{787}{20250}&\frac{13628448896}{58629571875}&\frac{1762}{11025}&-\frac{6}{145}&\frac{223}{18750}&-\frac{302}{183375}\\ \frac{737}{9000}&\frac{1446041816}{6514396875}&\frac{2601}{9800}&\frac{17}{232}&-\frac{27}{12500}&\frac{9}{163000}\\ \frac{1186}{30375}&\frac{40568406016}{175888715625}&\frac{2584}{11025}&\frac{832}{3915}&\frac{818}{9375}&-\frac{704}{183375}\\ \frac{29}{648}&\frac{19808792}{93807315}&\frac{1025}{3528}&\frac{25}{232}&\frac{17}{60}&\frac{733}{11736}\end{bmatrix}\begin{bmatrix}f_n\\ f_{n+\frac{27}{190}}\\ f_{n+\frac{2}{5}}\\ f_{n+\frac{3}{5}}\\ f_{n+\frac{4}{5}}\\ f_{n+1}\end{bmatrix}\Bigg\} \quad (3.4)$$

Expanding (3.4) in Taylor series gives,

$$\begin{bmatrix}\sum_{j=0}^{\infty}\left(\frac{27h}{190}\right)^j\gamma_n^j-\gamma_n-\frac{8352390951}{158470336000}-\sum_{j=o}^{\infty}\frac{h^{j+1}}{j!}\gamma_n^{j+1}\left\{\frac{5916138237}{55010462500}\left\langle\frac{27}{190}\right\rangle-\frac{27030145581}{776504646400}\left\langle\frac{2}{5}\right\rangle+\frac{280954413}{11489099360}\left\langle\frac{3}{5}\right\rangle\right.\\ \left.-\frac{36774910197}{3961758400000}\left\langle\frac{4}{5}\right\rangle+\frac{4816554759}{3228833096000}\langle 1\rangle\right\}\\ \sum_{j=0}^{\infty}\left(\frac{2h}{5}\right)^j\gamma_n^j-\gamma_n-\frac{787}{20250}-\sum_{j=o}^{\infty}\frac{h^{j+1}}{j!}\gamma_n^{j+1}\left\{\frac{13628448896}{58629571875}\left\langle\frac{27}{190}\right\rangle+\frac{1762}{11025}\left\langle\frac{2}{5}\right\rangle-\frac{6}{145}\left\langle\frac{3}{5}\right\rangle+\frac{223}{18750}\left\langle\frac{4}{5}\right\rangle-\frac{302}{183375}\langle 1\rangle\right\}\\ \sum_{j=0}^{\infty}\left(\frac{3h}{5}\right)^j\gamma_n^j-\gamma_n-\frac{737}{9000}-\sum_{j=o}^{\infty}\frac{h^{j+1}}{j!}\gamma_n^{j+1}\left\{\frac{1446041816}{6514396875}\left\langle\frac{27}{190}\right\rangle+\frac{2601}{9800}\left\langle\frac{2}{5}\right\rangle+\frac{17}{232}\left\langle\frac{3}{5}\right\rangle-\frac{27}{12500}\left\langle\frac{4}{5}\right\rangle+\frac{9}{163000}\langle 1\rangle\right\}\\ \sum_{j=0}^{\infty}\left(\frac{4h}{5}\right)^j\gamma_n^j-\gamma_n-\frac{1186}{30375}-\sum_{j=o}^{\infty}\frac{h^{j+1}}{j!}\gamma_n^{j+1}\left\{\frac{40568406016}{175888715625}\left\langle\frac{27}{190}\right\rangle+\frac{2584}{11025}\left\langle\frac{2}{5}\right\rangle+\frac{832}{3915}\left\langle\frac{3}{5}\right\rangle+\frac{818}{9375}\left\langle\frac{4}{5}\right\rangle-\frac{704}{183375}\langle 1\rangle\right\}\\ \sum_{j=0}^{\infty}(h)^j\gamma_n^j-\gamma_n-\frac{29}{648}-\sum_{j=o}^{\infty}\frac{h^{j+1}}{j!}\gamma_n^{j+1}\left\{\frac{19808792}{93807315}\left\langle\frac{27}{190}\right\rangle+\frac{1025}{3528}\left\langle\frac{2}{5}\right\rangle+\frac{25}{232}\left\langle\frac{3}{5}\right\rangle+\frac{17}{60}\left\langle\frac{4}{5}\right\rangle+\frac{733}{11736}\langle 1\rangle\right\}\end{bmatrix}=\begin{bmatrix}0\\0\\0\\0\\0\end{bmatrix} \quad (3.5)$$

Equating the coefficients of the Taylor series expansion to zero yields,

$$\bar{c}_0=\bar{c}_1=\bar{c}_2=\bar{c}_3=\bar{c}_4=\bar{c}_5=\bar{c}_6=0,$$
$$\bar{c}_7=\left[-7.9792\times10^{-08}\quad 5.1738\times10^{-08}\quad 3.3383\times10^{-09}\quad 6.7297\times10^{-08}\quad 1.30190\times10^{-09}\right]$$

Therefore, the OBNM is of uniform order six.

3.2. Consistency of OBNM

Definition 3.2: The numerical method OBNM is said to be consistent if it fulfills the subsequent conditions;

a. the order $p\geq 1$,

b. $\sum_{j=0}^{k}\alpha_j=0$, and

c. $\rho'(1)=\sigma(1)$

Now that the order $p\geq 6$, therefore, OBNM is consistent by definition 3.2 (Areo et al., 2024).

3.3. Zero Stability of OBNM

Definition 3.3: The OBNM is said to be zero-stable, if the roots $z_s, s=1,2,\cdots,k$ of the first characteristic polynomial $\rho(z)$ defined by $\rho(z)=\det\left(z\mathrm{K}^{(0)}-\Omega\right)$ satisfies $|z_s|\le 1$ and every root satisfying $|z_s|=0$ have multiplicity not exceeding the order of the differential equation. Moreover $h\to 0$, $\rho(z)=z^{r-\mu}(z-1)^{\mu}$, as where μ is the order of the differential equation, r is the order of the matrices $\mathrm{K}^{(0)}$ and Ω, (Adewale and Sabo, 2023).

Then, by definition 3.3, the zero-stability of OBNM gives,

$$\rho(z)=\left|z\begin{bmatrix}1&0&0&0&0\\0&1&0&0&0\\0&0&1&0&0\\0&0&0&1&0\\0&0&0&0&1\end{bmatrix}-\begin{bmatrix}0&0&0&0&1\\0&0&0&0&1\\0&0&0&0&1\\0&0&0&0&1\\0&0&0&0&1\end{bmatrix}\right|=0 \tag{3.6}$$

Solving for the values of $z_1, z_2, z_3, z_4=z_5$ in equation (3.6)

$\rho(z)=z^4(z-1)=0\Rightarrow z_1=z_2=z_3=z_4=z_5=0$. Therefore, the OBNM is zero-stable.

3.4. Convergence of OBNM

An OBNM is convergent by consequence of Dahlquist theorem presented in theorem 3.1.

Theorem 3.1: The necessary and sufficient conditions for OBNM is that, it must be consistent and zero-stable (Adewale and Sabo, 2023).

3.5. Absolute Stability of OBNM

Definition 3.4: Region of absolute stability is a region in the complex z plane, where $z=\lambda h$. It is defined as those values of such that the numerical solutions of $\gamma'=-\lambda\gamma$ satisfy $\gamma_j\to 0$ as $j\to\infty$ for any initial condition (Adewale et al., 2024). The boundary locus method were applied to determine the region of absolute stability of OBNM together with the test equation

$$\gamma'=-\lambda\gamma \tag{3.7}$$

Is used together with the OBNM. This gives

$$\mathrm{K}^{(0)}\mathrm{X}_m(w)=\Omega\gamma_n(w)-h\psi\mathrm{P}\gamma_n(w)-h\vartheta\Psi\mathrm{Y}_n(w) \tag{3.8}$$

Thus

$$\bar{h}(w)=-\frac{\mathrm{K}^{(0)}\mathrm{X}_n(w)-\Omega\gamma_n(w)}{\mathrm{P}\mathrm{Y}_n(w)+\Psi\mathrm{Y}_n(w)} \tag{3.9}$$

Since $\bar{h}$ given by $\bar{h}=\lambda h$ and $w=e^{i\theta}$. Equation (3.9) is the characteristics/stability polynomial of an optimization method, which is given by

$$\left.\begin{aligned}\bar{h}(w)=&\left(-\frac{163}{2850000}w^4-\frac{9}{237500}w^5\right)h^5+\left(-\frac{11083}{8550000}w^4+\frac{1453}{1425000}w^4\right)h^4+\left(-\frac{9001}{570000}w^4-\frac{7769}{570000}w^5\right)h^3\\&+\left(\frac{769}{7125}w^5-\frac{1117}{9500}w^4\right)h^2+\left(-\frac{559}{1140}w^5-\frac{581}{1140}w^4\right)h-w^4+w^5\end{aligned}\right\} \quad (3.10)$$

This gives the region of absolute stability presented in figure 3.1 below.

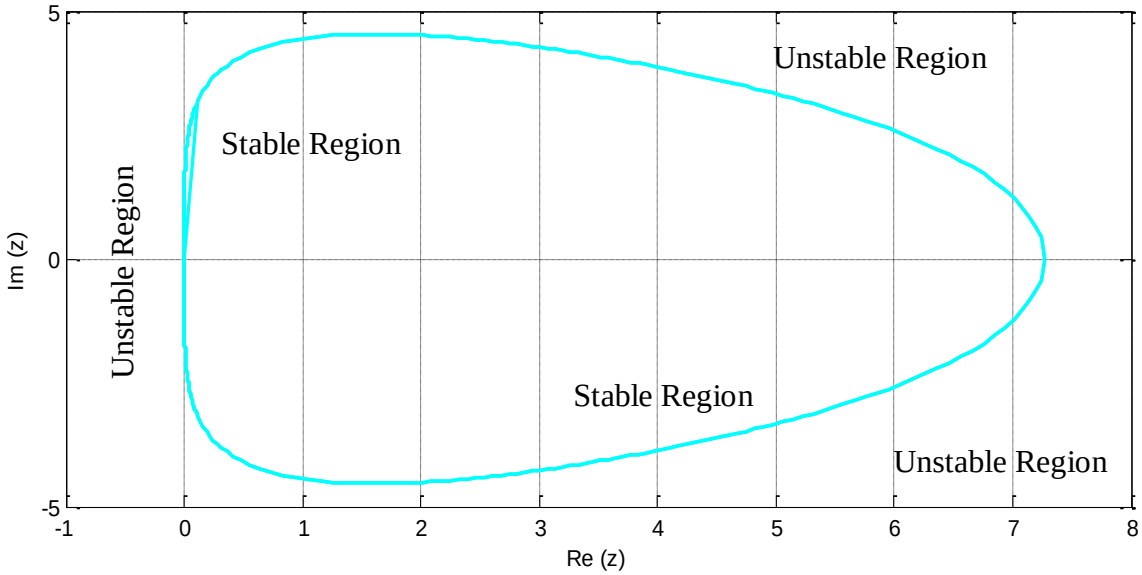


Figure 3.1. Region of Absolute stability of OBNM.

The region of absolute stability of OBNM in figure 3.1 is A-stable, since it contains the left half plane of the enclosed figure.

4.0. Numerical Application of Optimization-Based Numerical Method (OBNM)

The newly derived the Optimization-Based Numerical Method (OBNM) shall be applied on five real life modelled ordinary differential equations problems and the results are tabulated and graphical shown the comparison of absolute error with the following formula;

$$AErr = |Ana - App| \quad (4.1)$$

where AErr is the Absolute Error, Ana is the Analytical Solution and App is the Approximate Solution.

Example 4.1: (Newton's Law of Cooling)

A hot metal rod is heated to 150°C and placed in a room maintained at 30°C. The cooling rate is proportional to the difference between the rod's temperature and the room temperature. If the cooling constant is $0.08\,\text{min}^{-1}$, determine the temperature after a time t minutes. The Newton's Law of Cooling equations is modelled as ordinary differential equation as

$$\frac{d\gamma}{dt} = -0.08(\gamma - 30),\ \gamma(0) = 150 \quad (4.2)$$

With analytical solution given by

$$\gamma(t) = 30 + 120\exp(-0.08t) \tag{4.3}$$

Source: [Çengel & Ghajar, (2015)].

Example 4.2: (Radioactive Decay)

A radioactive sample initially contains 250g of a radioactive substance. The decay rate is proportional to the amount remaining. The example 4.2 is modelled as ordinary differential equation of the form

$$\frac{dD}{dt} = -0.06D,\ D(0) = 250 \tag{4.4}$$

The analytical solution of the Radioactive Decay given as

$$D(t) = 250\exp(-0.06t) \tag{4.5}$$

Source: [L'Annunziata, (2012)].

Example 4.3: (Drug Elimination)

A patient receives 800 mg of medication. The drug leaves the bloodstream at a rate proportional to the amount present. The ordinary differential equation is modelled as

$$\frac{dA}{dt} = -0.25A,\ A(0) = 800 \tag{4.6}$$

whose analytical solution is given by

$$A(t) = 800\exp(-0.25t) \tag{4.7}$$

Source: [L'Annunziata, (2012)].

Example 4.4: (Heating of Water)

A container of water is initially at 20°C and is placed in an oven maintained at 90°C. The Heating of Water differential equation is modelled as

$$\frac{dW}{dt} = 0.12(90 - W),\ W(0) = 20 \tag{4.8}$$

The analytical solution gives

$$W(t) = 90 - 70\exp(-0.12t) \tag{4.9}$$

Source: [Çengel & Ghajar, (2015)]

Example 4.5: (Changing a Capacitor)

A capacitor is connected to a 12 Voltage DC power supply through a resistor. The capacitor is initially uncharged and the modelled differential equation is given by

$$\frac{dV}{dt} = \frac{12 - V}{4},\ V(0) = 0 \tag{4.10}$$

with analytical solution is given by

$$W(t) = 90 - 70\exp(-0.12t) \tag{4.11}$$

Source: [Halliday, et al., 2025]

Table 4.1. Numerical Result of Example 4.1.

t	**Ana**	**App**	**AErr**
0.1	149.04382978044727564000	149.04382978044727564000	0.0000×10^{00}
0.2	148.09527840663421382000	148.09527840663421382000	0.0000×10^{00}
0.3	147.15428517094911762000	147.15428517094911762000	0.0000×10^{00}
0.4	146.22078984950371014000	146.22078984950371014000	0.0000×10^{00}
0.5	145.29473269827878513000	145.29473269827878512000	1.0000×10^{-17}
0.6	144.37605444930056935000	144.37605444930056933000	2.0000×10^{-17}
0.7	143.46469630684755201000	143.46469630684755198000	3.0000×10^{-17}
0.8	142.56059994368753853000	142.56059994368753850000	3.0000×10^{-17}
0.9	141.66370749734468781000	141.66370749734468778000	3.0000×10^{-17}
1.0	140.77396156639629395000	140.77396156639629391000	4.0000×10^{-17}
1.1	139.89130520679907566000	139.89130520679907563000	3.0000×10^{-17}
1.2	139.01568192824473805000	139.01568192824473800000	5.0000×10^{-17}
1.3	138.14703569054457358000	138.14703569054457353000	5.000×10^{-17}
1.4	137.28531090004287089000	137.28531090004287084000	5.0000×10^{-17}
1.5	136.43045240605890186000	136.43045240605890181000	5.0000×10^{-17}
1.6	135.58240549735725919000	135.58240549735725914000	5.0000×10^{-17}
1.7	134.74111589864631867000	134.74111589864631862000	5.0000×10^{-17}
1.8	133.90652976710460202000	133.90652976710460196000	6.0000×10^{-17}
1.9	133.07859368893481788000	133.07859368893481782000	6.0000×10^{-17}
2.0	132.25725467594536062000	132.25725467594536054000	8.0000×10^{-17}

Table 4.2. Numerical Result of Example 4.2.

t	**Ana**	**App**	**AErr**
0.1	248.50449101348381618000	248.50449101348381619000	1.0000×10^{-17}
0.2	247.01792821548263502000	247.01792821548263504000	2.0000×10^{-17}
0.3	245.54025808957517950000	245.54025808957517952000	2.0000×10^{-17}
0.4	244.07142743947732838000	244.07142743947732841000	3.0000×10^{-17}
0.5	242.61138338712704423000	242.61138338712704427000	4.0000×10^{-17}
0.6	241.16007337078075751000	241.16007337078075756000	5.0000×10^{-17}
0.7	239.71744514312113808000	239.71744514312113813000	5.0000×10^{-17}
0.8	238.28344676937618614000	238.28344676937618621000	7.0000×10^{-17}
0.9	236.85802662544957488000	236.85802662544957496000	8.000×10^{-17}
1.0	235.44113339606217738000	235.44113339606217747000	9.0000×10^{-17}

1.1	234.03271607290471104000	234.03271607290471114000	1.0000×10^{-16}
1.2	232.63272395280143294000	232.63272395280143304000	1.0000×10^{-16}
1.3	231.24110663588482002000	231.24110663588482013000	1.1000×10^{-16}
1.4	229.85781402378116844000	229.85781402378116856000	1.2000×10^{-16}
1.5	228.48279631780704669000	228.48279631780704681000	1.2000×10^{-16}
1.6	227.11600401717653760000	227.11600401717653773000	1.3000×10^{-16}
1.7	225.75738791721920474000	225.75738791721920488000	1.4000×10^{-16}
1.8	224.40689910760871892000	224.40689910760871907000	1.5000×10^{-16}
1.9	223.06448897060208120000	223.06448897060208136000	1.6000×10^{-16}
2.0	221.73010917928937888000	221.73010917928937904000	1.6000×10^{-16}

Table 4.3. Numerical Result of Example 4.3.

t	**Ana**	**App**	**AErr**
0.1	780.24792962266613490000	780.24792962266613426000	6.4000×10^{-16}
0.2	760.98353960057120727000	760.98353960057120602000	1.2500×10^{-15}
0.3	742.19478906284231378000	742.19478906284231194000	1.8400×10^{-15}
0.4	723.86993442876765853000	723.86993442876765614000	2.3900×10^{-15}
0.5	705.99752206767632229000	705.99752206767631938000	2.9100×10^{-15}
0.6	688.56638114004624578000	688.56638114004624237000	3.4100×10^{-15}
0.7	671.56561661536588675000	671.56561661536588287000	3.8800×10^{-15}
0.8	654.98460246238548694000	654.98460246238548260000	4.3400×10^{-15}
0.9	638.81297500750163427000	638.81297500750162951000	4.7600×10^{-15}
1.0	623.04062645712389460000	623.04062645712388944000	5.1600×10^{-15}
1.1	607.65769857997478102000	607.65769857997477549000	5.5300×10^{-15}
1.2	592.65457654537429286000	592.65457654537428697000	5.8900×10^{-15}
1.3	578.02188291365775130000	578.02188291365774508000	6.2200×10^{-15}
1.4	563.75047177497074748000	563.75047177497074095000	6.5300×10^{-15}
1.5	549.83142303277775884000	549.83142303277775201000	6.8300×10^{-15}
1.6	536.25603682851144059000	536.25603682851143349000	7.1000×10^{-15}
1.7	523.01582810387781681000	523.01582810387780945000	7.3600×10^{-15}
1.8	510.10252129741863451000	510.10252129741862692000	7.5900×10^{-15}
1.9	497.50804517201605996000	497.50804517201605214000	7.8200×10^{-15}
2.0	485.22452777010673888000	485.22452777010673086000	8.0200×10^{-15}

Table 4.4. Numerical Result of Example 4.4.

t	**Ana**	**App**	**AErr**
0.1	20.83498009966486219300	20.83498009966486219300	0.0000×10^{00}
0.2	21.66000031694634805400	21.66000031694634805400	0.0000×10^{00}
0.3	22.47517945618138789700	22.47517945618138789500	2.0000×10^{-18}

0.4	23.28063490457466788000	23.28063490457466787900	1.0000×10^{-18}
0.5	24.07648264910259033200	24.07648264910259033100	1.0000×10^{-18}
0.6	24.86283729321559877800	24.86283729321559877600	2.0000×10^{-18}
0.7	25.63981207334127283700	25.63981207334127283500	2.0000×10^{-18}
0.8	26.40751887519056947100	26.40751887519056946900	2.0000×10^{-18}
0.9	27.16606824986955870200	27.16606824986955869800	4.0000×10^{-18}
1.0	27.91556942979897391300	27.91556942979897390800	5.0000×10^{-18}
1.1	28.66561303444386919700	28.66561303444386919100	6.0000×10^{-18}
1.2	29.38785763585564882100	29.38785763585564881500	6.0000×10^{-18}
1.3	30.11085667402870691100	30.11085667402870690500	6.0000×10^{-18}
1.4	30.82523157207388872200	30.82523157207388871400	8.0000×10^{-18}
1.5	31.53108520121095850800	31.53108520121095850000	8.0000×10^{-18}
1.6	32.22851920558223293400	32.22851920558223292500	9.0000×10^{-18}
1.7	32.91763401688951320900	32.91763401688951319900	1.0000×10^{-17}
1.8	33.59852886885642368900	33.59852886885642367700	1.2000×10^{-17}
1.9	34.27130181151823956200	34.27130181151823954900	1.3000×10^{-17}
2.0	34.93604972534126135500	34.93604972534126133900	1.6000×10^{-17}

Table 4.5. Numerical Result of Example 4.5.

t	**Ana**	**App**	**AErr**
0.1	0.29628105566000797600	0.29628105566000798587	9.8700×10^{-18}
0.2	0.58524690599143189100	0.58524690599143190922	1.8220×10^{-17}
0.3	0.86707816405736529300	0.86707816405736532019	2.7190×10^{-17}
0.4	1.14195098356848512200	1.14195098356848515690	3.4900×10^{-17}
0.5	1.41003716898485516600	1.41003716898485520820	4.2200×10^{-17}
0.6	1.67150428289930631300	1.67150428289930636300	5.0000×10^{-17}
0.7	1.92651575076951169900	1.92651575076951175530	5.6300×10^{-17}
0.8	2.17523096306421769600	2.17523096306421775910	6.3100×10^{-17}
0.9	2.41780537488747548590	2.41780537488747555520	6.9300×10^{-17}
1.0	2.65439060314314158100	2.65439060314314165600	7.5000×10^{-17}
1.1	2.88513452130037828460	2.88513452130037836500	8.0400×10^{-17}
1.2	3.11018135181938560720	3.11018135181938569260	8.5400×10^{-17}
1.3	3.32967175629513373060	3.32967175629513382050	8.9900×10^{-17}
1.4	3.54374292337543878780	3.54374292337543888230	9.4500×10^{-17}
1.5	3.75252865450833361740	3.75252865450833371620	9.8800×10^{-17}
1.6	3.95615944757232839110	3.95615944757232849380	1.0270×10^{-16}
1.7	4.15476257844183274790	4.15476257844183285420	1.0630×10^{-16}
1.8	4.34846218053872048230	4.34846218053872059210	1.0980×10^{-16}
1.9	4.53737932241975910060	4.53737932241975921350	1.1290×10^{-16}
2.0	4.72163208344839891680	4.72163208344839903250	1.1570×10^{-16}

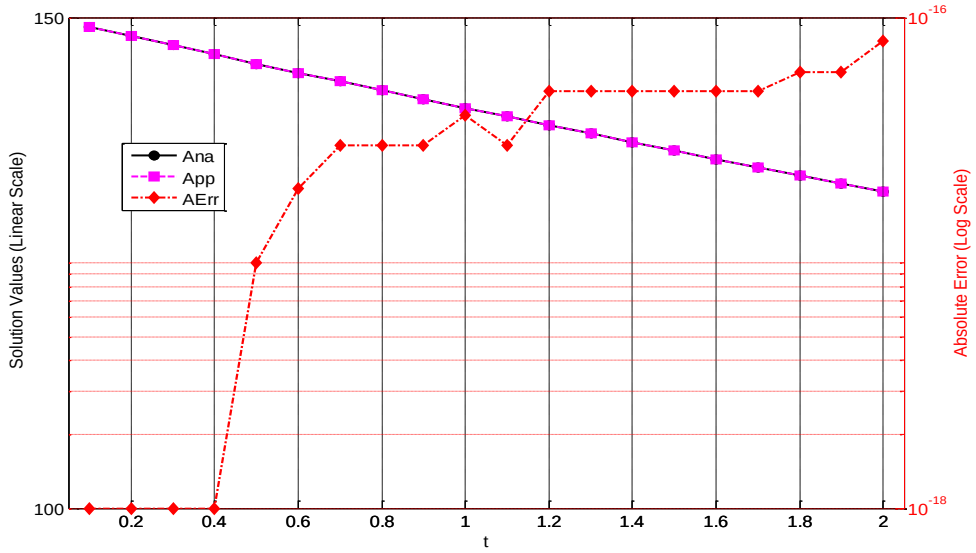


Figure 4.1. Graphical Curve of Table 4.1.

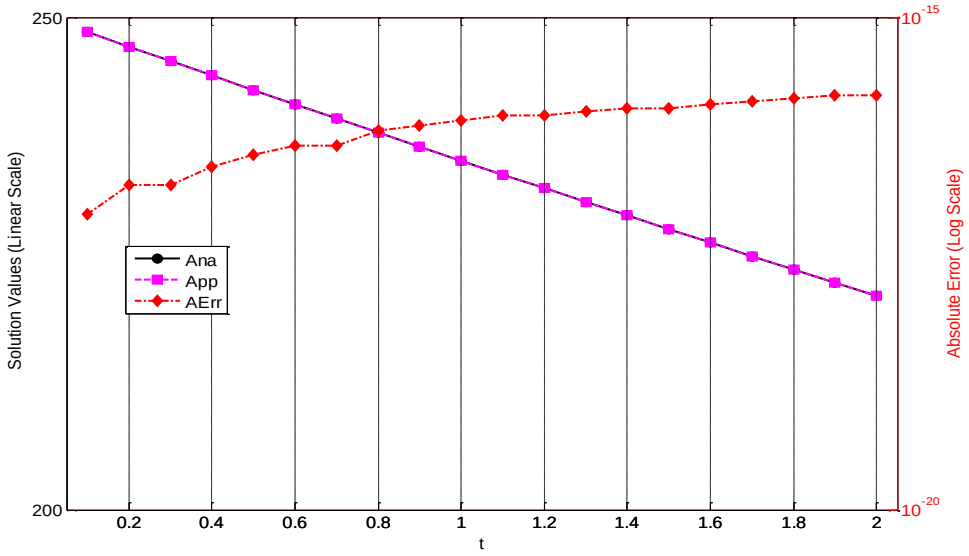


Figure 4.2. Graphical Curve of Table 4.2.

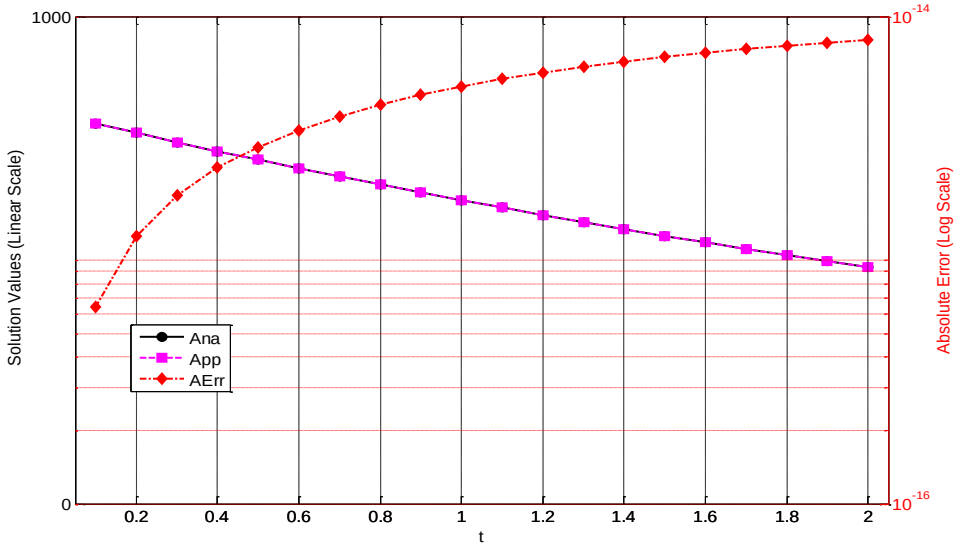


Figure 4.3. Graphical Curve of Table 4.3.

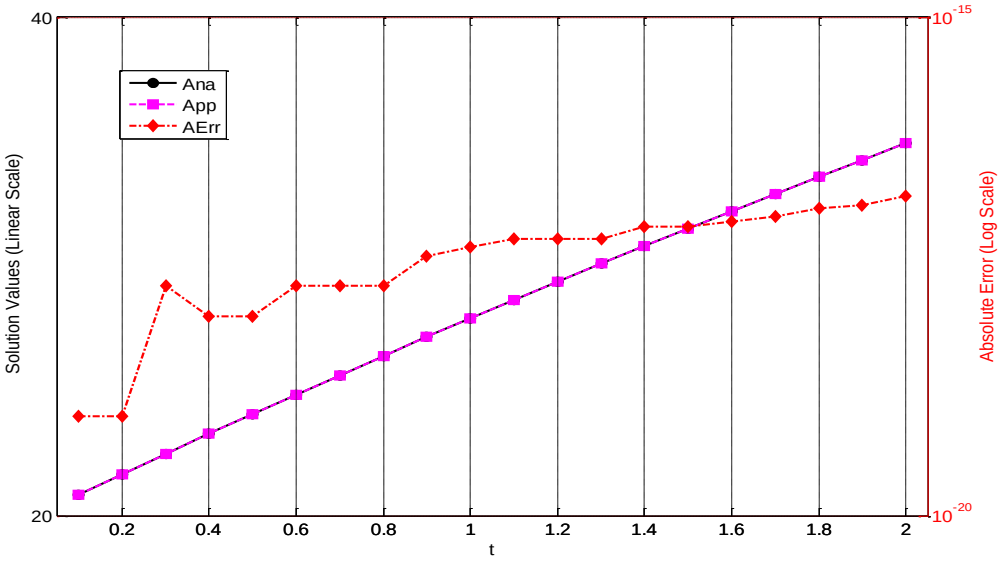


Figure 4.4. Graphical Curve of Table 4.4.

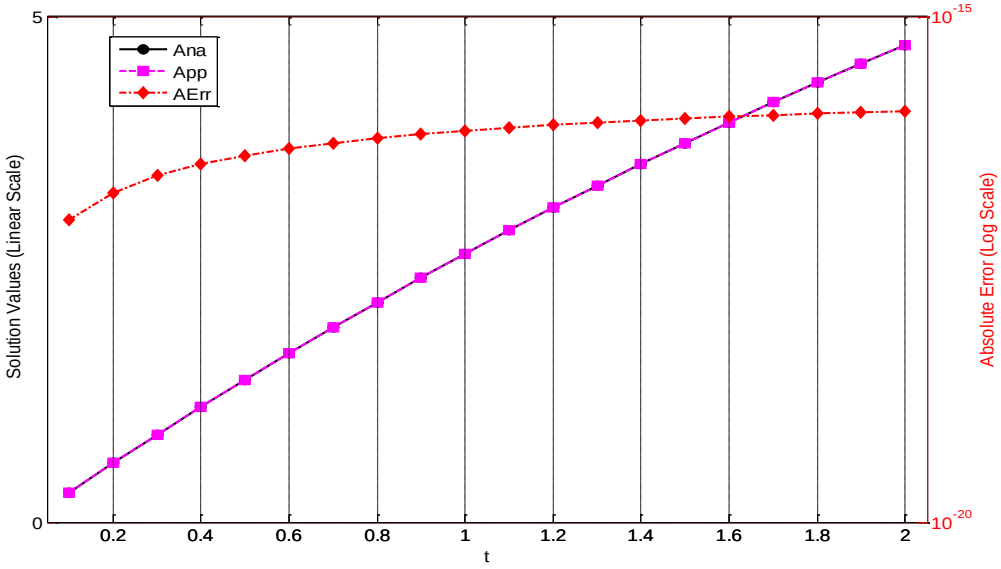


Figure 4.5. Graphical Curve of Table 4.5.

5.0. Discussion of Results

As presented in Table 4.1 and illustrated in Figure 4.1, this problem models the cooling of a hot metal rod from 150°C in a 30°C room. The analytical solution starts at 149.04 and decays smoothly to 132.26 by $t = 2.0$, reflecting the expected exponential cooling behaviour. The OBNM approximate solution matches the analytical solution so closely that the two columns are virtually identical. The absolute errors are zero for the first four evaluation points $(t = 0.1)$ to $(t = 0.4)$ and then rise only to the order of 10^{-17} for the remaining points, peaking at 8.0000×10^{-17} at $(t = 2.0)$. These values are at the level of double-precision machine round-off, meaning the method reproduces the analytical solution to the limits of the computer's floating-point representation. Figure 4.1 clearly shows the two solution curves superimposed, with the error curve (plotted on a logarithmic right axis) lying far below the solution curves, confirming the near-exact accuracy of OBNM for first-order linear decay-type problems. This example sets the benchmark against which the subsequent examples are compared.

Following the same format, Example 4.2 (see Table 4.2 and Figure 4.2), this example concerns the decay of an initial 250 g radioactive sample. The analytical solution decreases from 248.50 at $(t = 0.1)$ to 221.73 at $(t = 2.0)$, consistent with exponential decay. The OBNM results again track the analytical values to an extraordinary degree. The absolute errors start at 1.0000×10^{-17} and increase gradually to 1.6000×10^{-16} at $(t = 2.0)$. Although the errors are slightly larger than those in Table 4.1, they remain at machine-precision level and show a smooth, monotonic increase with τ, which is the normal accumulation of round-off error in a fixed-step integration. Figure 4.2 illustrates that the analytical and approximate curves are indistinguishable over the entire interval, while the error curve remains many orders of magnitude below the solution values. This confirms that OBNM handles exponential decay with the same high accuracy as the cooling problem in Example 4.1.

Adopting the same presentation, the modelled example 4.3 problem elimination of an 800 mg dose of medication from the bloodstream. The analytical solution decays from 780.25 at $(t = 0.1)$ to 485.22 at $(t = 2.0)$. The OBNM approximate solution follows the analytical solution extremely closely, with absolute errors ranging from 6.4000×10^{-16} to 8.0200×10^{-15}. These errors are slightly larger than those in Table 4.1 and Table 4.2 because the solution values themselves are larger (of order 102102 to 103103), so a fixed relative error translates into a larger absolute error. Even so, the errors remain at the 10^{-15} level, which is essentially machine precision for numbers of this magnitude. The error grows smoothly and monotonically with τ, reflecting the gradual accumulation of round-off error. Figure 4.3 shows the two solution curves completely overlapping and the error curve staying several orders of magnitude below the solution curve, confirming the accuracy and stability of OBNM for this pharmacokinetic model. Example 4.4 which is Heating of Water with the results in (Table 4.4 and Figure 4.4), this example models the heating of water from 20°C toward an oven temperature of 90°C. The analytical solution reflecting the expected approach to the equilibrium temperature. The OBNM approximate solution matches the analytical solution almost perfectly. The absolute errors are zero gradually increasing. These errors are even smaller than those in Table 4.1, which is remarkable given that the solution is growing rather than decaying. The growth of the error with *t* is smooth and monotonic and the overall error is at the limit of double-precision arithmetic. Figure 4.4 confirms that the analytical and approximate curves coincide completely, with the error curve lying far below them.

The Example 4.5 modelled Charging a Capacitor with the results in Table 4.5 and Figure 4.5 explain the charging of a capacitor from an initial uncharged state toward a 12 V supply. The analytical solution rises from 0.296 to 4.722, following the characteristic exponential approach to the steady-state voltage. The OBNM approximate solution follows the analytical solution with absolute errors ranging from 9.8700×10^{-18} to 1.1570×10^{-16} at. Although the solution values are much smaller than in the previous examples (of order 100100), again demonstrating machine-precision accuracy comparable to that observed in Table 4.1. The error grows smoothly and monotonically with *t* and Figure 4.5 shows the analytical and approximate curves perfectly superimposed, with the error curve many orders of magnitude below the solution curve.

6.0. Summary and Conclusion

This study formulated and analyzed an Optimization-Based Numerical Method (OBNM) for solving first-order ordinary differential equations that model real-world scientific and engineering phenomena. The method was

derived from a power series polynomial approximation using interpolation at a single point and collocation at six points, including an optimization point obtained by minimizing the truncation error. The resulting continuous formulation was evaluated at selected grid points to produce a block hybrid scheme with constant coefficients.

The theoretical properties of the method were rigorously established: the order and error constant analysis confirmed a high order of accuracy, consistency was verified since the order exceeds one and the characteristic polynomials satisfy the required conditions, zero-stability was demonstrated through the roots of the first characteristic polynomial lying within the unit circle, convergence followed from the Dahlquist theorem as a consequence of consistency and zero-stability, and absolute stability was established using the boundary locus method, with the region of absolute stability enclosing the left half-plane, confirming that the method is A-stable. These properties collectively indicate that the OBNM is a robust and reliable numerical scheme suitable for stiff and non-stiff first-order ODE problems.

The OBNM was applied to five benchmark problems representing Newton's law of cooling, radioactive decay, drug elimination, heating of water, and capacitor charging and its performance was evaluated against analytical solutions using absolute error as the metric. The numerical results, presented in tables and graphs, showed that the approximate solutions were virtually indistinguishable from the analytical solutions, with absolute errors at the level of double-precision machine round-off. The error growth was smooth and monotonic across all examples and the graphical comparisons confirmed that the error curves remained many orders of magnitude below the solution curves. These findings demonstrate that the OBNM achieves near-exact accuracy for first-order linear ODEs of the decay and growth type, while its established consistency, zero-stability, convergence and A-stability guarantee dependable performance. The method therefore offers a highly accurate, stable, and computationally efficient alternative for solving ODE models in chemistry, physics, engineering, and applied mathematics and it is recommended for extension to systems of ODEs and higher-order problems in future work.

7.0. Suggestions for Further Research

Building on these findings, the following are suggestions for further research.

1. Further research could extend the OBNM to coupled systems of first-order ODEs, such as predator–prey, SIR epidemic and coupled chemical kinetics models.

2. Further research could extend the OBNM to second- and higher-order initial value problems, including oscillatory and vibratory systems.

3. Further research could apply the OBNM to genuinely stiff and nonlinear benchmark problems, such as Robertson's chemical kinetics and the Van der Pol equation, to validate the A-stability claims under real stiffness.

4. Further research could develop a variable-step or adaptive version of the OBNM with local error estimation and step control to improve long-time integration accuracy.

5. Further research could provide rigorous global error bounds under nonlinear Lipschitz conditions and compare alternative optimization criteria for selecting the optimal point.

6. Further research could benchmark the OBNM against established solvers (RK45, BDF, Radau IIA) and other optimized hybrid block methods on identical test problems, measuring accuracy, CPU time, and stability-region coverage.

7. Further research could extend the OBNM framework to fractional-order and delay differential equations, broadening its applicability to memory-dependent and pharmacokinetic systems.

8. Further research could apply the OBNM to coupled multi-physics models and embed it within engineering design optimization loops that require repeated ODE solves.

9. Further research could produce an open-source implementation of the OBNM with documented coefficient matrices to support reproducibility and adoption.

Declarations

Source of Funding

This study received no specific grant from any funding agency in the public, commercial, or not-for-profit sectors.

Competing Interests Statement

The authors affirm that they have no competing interests that may have affected the findings or interpretations outlined in this study.

Consent for publication

The authors declare that they consented to the publication of this study.

Authors' contributions

All the authors made an equal contribution in the Conception and design of the work, Data collection, Drafting the article, and Critical revision of the article. All the authors have read and approved the final copy of the manuscript.

Institutional Review Board Statement

Not applicable for this study.

References

Abdelrahim, R., Omar, Z., & Kuboye, J.O. (2016). New hybrid block method with three off-step points for solving first-order ordinary differential equations. Am J Appl Sci., 1(3): 3–6.

Adewale, A.J., & Sabo, J. (2023). The physical simulation of oscillatory differential equations of mass in motion. American University of Nigeria, 1st International Conference Proceeding, Pages 544–560.

Adewale, A.J., Sabo, J., Solomon, E., & Aliyu, M. (2024). Derivation and analysis of block hybrid method for solving initial value problems in oscillatory differential equations. American University of Nigeria, 2nd International Conference Proceeding, Pages 1–12.

Ahmad, M. (2020). Solution of Some Optimization Problems by Numerical Methods. IOSR Journal of Mathematics (IOSR-JM), 16(6): 01–06. https://doi.org/10.9790/5728-1606010106.

Akinfenwa, O.A., Abdulganiy, R.I., Akinnukawe, B.I., & Okunuga, S.A. (2020). Seventh-order hybrid block method for solution of first-order stiff systems of initial value problems. Journal of the Egyptian Mathematical Society, 28(34): 1–11.

Akinnukawe, B.I. (2025). Optimized algorithm for the numerical solution of third-order ordinary differential equations. LASU Postgraduate School Journal, 2(1): 228–239. https://doi.org/10.5281/zenodo.16879004.

Aljassas, S.M., & Al-Jilawi, A.S. (2023). A numerical technique for solving optimization problems. Wasit Journal for Pure Science, 2(4): 1–11. https://doi.org/10.31185/wjps.92.

Alzaid, S.S., Shaw, P.K., & Kumar, S. (2022). A study of Ralston's cubic convergence with the application of population growth model. AIMS Mathematics, 7(6): 11320–11344.

Areo, E.A., Olabode, B.T., Gbenro, S.O., & Momoh, A.L. (2024). One-step three-parameter optimized hybrid block method for solving first-order initial value problems of ODEs. Journal of Mathematical Analysis and Modeling, 4(3): 41–59. https://doi.org/10.48185/jmam.v4i3.970.

Atkins, P., & de Paula, J. (2014). Physical chemistry (10th Ed.). Oxford University Press.

Butcher, J.C. (2016). Numerical methods for ordinary differential equations (3rd Ed.). John Wiley & Sons Ltd.

Çengel, Y.A., & Ghajar, A.J. (2015). Heat and mass transfer: Fundamentals and applications (5th Ed.). McGraw-Hill Education.

Chan, C.K., Dumka, P., Sonawane, C., Singh, S., & Varshaney, D. (2025). Numerical solution of ordinary differential equations using Newton–Raphson method with NumPy and Autograd: Accuracy, convergence, and performance analysis. International Journal of Innovative Research and Scientific Studies, 8(3): 4293–4303. https://doi.org/10.53894/ijirss.v8i3.7504.

Gavin, H.P. (2019). Constrained Optimization [Course Notes]. Department of Civil and Environmental Engineering, Duke University.

Gbenro, S.O. (2025). Optimized hybrid block methods with high efficiency for the solution of first-order ordinary differential equations. Asian Research Journal of Mathematics, 21(2): 1–11. https://doi.org/10.9734/arjom/2025/v21i2888.

Halliday, D., Resnick, R., & Walker, J. (2014). Fundamentals of physics (10th Ed.). Wiley.

Kumar, S., Shaw, P.K., Abdel-Aty, A.H., & Mahmoud, E.E. (2024). A numerical study on fractional differential equation with population growth model. Numerical Methods for Partial Differential Equations, 40(1): 23–41.

L'Annunziata, M.F. (Ed.) (2012). Handbook of radioactivity analysis (3rd Ed.). Academic Press.

Malins, A., & Lemoine, T. (2022). Radioactivedecay: A Python package for radioactive decay calculations. Journal of Open Source Software, 7(71): 331.

Peker, H.A., & Uysal, E. (2024). Application of the new general integral transform for Newton's law of cooling. The Eurasia Proceedings of Science, Technology, Engineering & Mathematics, Pages 216–223.

Petrović, M.J., Stanimirović, P.S., & Milovanović, G.V. (2025). Numerical analysis and optimization. Axioms, 14(4): 305. https://doi.org/10.3390/axioms14040305.

Sabo, J., Adewale, A.J., Ayinde, M.A., Umar, M.O., Akanbi, M.B., & Belgore, A.K. (2024). Numerical methods for solving first-order nonlinear differential equations using a linear block approach. American University of Nigeria, 2nd International Conference Proceeding, Pages 27–37.

Saha, P., Kushare, S.R., & Takate, A.M. (2025). Analytical solution of fractional Newton's law of cooling using Kushare transform. International Journal of Applied Mathematics, 38(1s): 12–29.

Widodo & Indarsih (2020). Drug elimination in two-compartment pharmacokinetic models with nonstandard finite difference approach. AIP Conference Proceedings.

Yakubu, S.D., & Sibanda, P. (2025). A novel one-step optimized hybrid block method for solving general second-order ordinary differential equations. Recent Advances in Natural Sciences, 3: 135. https://doi.org/10.61298/rans.2025.3.135.